

New periodic variable stars coincident with ROSAT sources discovered using SuperWASP

A.J. Norton¹, P.J. Wheatley², R.G. West³, C.A. Haswell¹, R.A. Street⁴, A. Collier Cameron⁵, D.J. Christian⁴, W.I. Clarkson⁶, B. Enoch¹, M. Gallaway¹, C. Hellier⁷, K. Horne⁵, J. Irwin⁸, S.R. Kane⁹, T.A. Lister⁷, J.P. Nicholas², N. Parley¹⁰, D. Pollacco⁴, R. Ryans⁴, I. Skillen¹¹, D.M. Wilson⁷

- ¹ Department of Physics and Astronomy, The Open University, Walton Hall, Milton Keynes MK7 6AA, U.K.
- ² Department of Physics, University of Warwick, Coventry CV4 7AL, U.K.
- ³ Department of Physics and Astronomy, University of Leicester, Leicester LE1 7RH, U.K.
- ⁴ Astrophysics Research Centre, Main Physics Building, School of Mathematics & Physics, Queen's University, University Road, Belfast BT7 1NN, U.K.
- ⁵ School of Physics and Astronomy, University of St. Andrews, North Haugh, St. Andrews, Fife KY16 9SS, U.K.
- ⁶ Space Telescope Science Institute, 3700 San Martin Drive, Baltimore, MD 21218, U.S.A.
- ⁷ Astrophysics Group, School of Chemistry & Physics, Keele University, Staffordshire ST5 5BG, U.K.
- ⁸ Institute of Astronomy, University of Cambridge, Madingley Road, Cambridge CB3 0HA, U.K.
- ⁹ Department of Physics, University of Florida, Gainesville, FL 32611-8440, U.S.A.
- ¹⁰ Planetary & Space Sciences Research Institute, The Open University, Walton Hall, Milton Keynes MK7 6AA, U.K.
- ¹¹ Isaac Newton Group of Telescopes, Apartado de Correos 321, E-38700 Santa Cruz de la Palma, Tenerife, Spain

Accepted 21 Feb 2007; Received 12 Jan 2007

Abstract. We present optical lightcurves of 428 periodic variable stars coincident with *ROSAT* X-ray sources, detected using the first run of the SuperWASP photometric survey. Only 68 of these were previously recognised as periodic variables. A further 30 of these objects are previously known pre-main sequence stars, for which we detect a modulation period for the first time. Amongst the newly identified periodic variables, many appear to be close eclipsing binaries, their X-ray emission is presumably the result of RS CVn type behaviour. Others are probably BY Dra stars, pre-main sequence stars and other rapid rotators displaying enhanced coronal activity. A number of previously catalogued pulsating variables (RR Lyr stars and Cepheids) coincident with X-ray sources are also seen, but we show that these are likely to be misclassifications. We identify four objects which are probable low mass eclipsing binary stars, based on their very red colour and light curve morphology.

Key words. stars: binaries: eclipsing – stars: rotation – stars: variables: general

1. Introduction

The SuperWASP project (Pollacco et al. 2006) is a wide field photometric survey designed to search for transiting exoplanets and other signatures of variability on timescales from minutes to months. In its first run during 2004, SuperWASP-N on La Palma was operated between May and September with five cameras, each of which has a $7.8^\circ \times 7.8^\circ$ field of view. The fields surveyed in 2004 comprise a strip of sky centred at declination $+28^\circ$ and extending to all right ascensions (excluding the galactic plane). Coverage is not uniform though, with some regions of sky better sampled than others. The resulting area covered was $\sim 10,000$ square degrees and comprised over 300,000 raw images. Photometry for all objects de-

tected was extracted using a 2.5 pixel aperture ($34''$ radius). As a result, the project produced unfiltered (white light) lightcurves of over 6.7 million stars in the magnitude range $V \sim 8 - 15$, totalling 12.9 billion data points. Because of the wide-field nature of the images, systematic errors in the lightcurves are present, but are largely removed using the SysREM algorithm from Tamuz et al. (2005). Plots showing the RMS precision of our data as a function of SuperWASP V magnitude, both before and after application of the SysREM algorithm, are shown in Collier Cameron et al. (2006a).

The 2004 survey allowed the identification of ~ 100 transiting exoplanet candidates, which we have reported in a series of papers (Christian et al. 2006, Clarkson et al. 2007, Kane et al. in preparation, Lister et al. 2007, Street et al. 2007, West et al. in preparation). The first con-

firmed planets resulting from this are reported by Collier Cameron et al. (2006b). These data also uncovered huge numbers of variable stars, many of which are previously unidentified. In this paper we discuss a small subset of these, namely those that are coincident with *ROSAT* X-ray sources. Our reasons for concentrating on the subset of variable sources which are X-ray sources are twofold. First, variable objects coincident with X-ray sources are likely to yield significant numbers of astrophysically important and interesting objects. Secondly, this provides a manageable number of objects with which to demonstrate the efficiency of SuperWASP for detecting variable objects other than transiting exoplanets. SuperWASP provides a significant increase in time coverage as compared to many single object studies and smaller photometric campaigns.

2. Period searching

The positions of objects in the SuperWASP archive are derived from the USNO-B1 catalogue (Monet et al. 2003). These positions were cross correlated against the *ROSAT* sky survey (1RXS; Voges et al. 1999, 2000) and pointed phase (2RXP; ROSAT 2000) catalogues, taking the uncertainty in position of each *ROSAT* source as its 3σ error radius, or $10''$, whichever was larger. This resulted in 4,562 matches between the positions of SuperWASP objects from our 2004 Northern hemisphere run and the positions of *ROSAT* sources. From this set of cross identifications, 3,558 SuperWASP lightcurves have more than 100 data points, and so were deemed to be suitable for period searching. A purpose written period search code was then run on these to identify periodic variables, coincident with X-ray sources.

The period search comprised two techniques. A CLEANed power spectrum was calculated, using the variable gain implementation of H. Lehto, and the strongest peaks within it identified. A period folding analysis was also performed, searching over periods from 20 minutes to half the lightcurve length in each case. Binning the data into 20 phase bins at each trial period, we calculated the reduced chi-squared of the folded lightcurve with respect to its mean flux and also the sum of the reduced chi-squareds of the data within each phase bin with respect to the mean flux in that bin. The most likely periods were then taken as those which maximised the difference between these two chi-squared values. This jointly minimised the dispersion within each phase bin and maximised the dispersion between the phase bins, in order to identify likely periods. Only those periods found in common between the CLEANed power spectrum and period folding technique (within a tolerance of 1%) were recorded. It was noted that a few systematic effects remain in the SuperWASP lightcurves, sometimes resulting in spurious periods being identified due to night-to-night variations. As a result, we ignored periods within 1% of one day and fractions thereof (i.e. $1d/2$, $1d/3$, $1d/4$, etc). We also rejected around 20 objects where several sources within a few arcminutes of each other each displayed sim-

ilar lightcurves with similar long term (tens of days) periodicities. These are believed to be artefacts due to remaining systematic errors in the extracted data. After this there remained 516 SuperWASP sources in this set for which periodic variability was identified, with periods ranging from less than 3h to more than 50d.

88 of these variable sources were noted to be duplicates of other stars in the list, recorded with slightly different positions (typically within 10 arcseconds) due to the large pixel size of the SuperWASP cameras. These arise where there are multiple USNO-B1 objects within a few arcseconds of each other, and the SuperWASP data resulting from different images are variously assigned to one of this small set of objects. Encouragingly, we detected the *same* period in the multiple SuperWASP lightcurves in each case. Most of these duplicates consisted of just two SuperWASP lightcurves corresponding to the same object, but in a couple of cases there were as many as five SuperWASP lightcurves corresponding to the same object, each with slightly different positions but showing the same periodicity. After removing these duplicates, there remained 428 unique objects showing periodic variability in their SuperWASP lightcurves and coincident with *ROSAT* X-ray sources.

3. Results

The positions of the 428 periodic SuperWASP objects were cross-correlated against the SIMBAD database. In order to account for the $34''$ radius photometry aperture used for our data, we searched for all objects in SIMBAD within twice this distance of the nominal SuperWASP position, and identified the most likely source of the variable signal in each case. As a result we identified 68 sources that have been previously recorded as periodic variable stars, of which 66 have periods given in the literature. These objects comprise 47 listed in the General Catalogue of Variable Stars, 17 discovered by the ROTSE (Robotic Optical Transient Search Experiment) survey (Akerlof et al. 2000), 2 discovered by the SAVS (Semi-Automatic Variability Search) survey (Maciejewski et al. 2004) and 2 objects (HD170451 and SAO46441) recently identified as W Uma type eclipsing binaries but not yet assigned GCVS designations. This set of 68 objects also includes two identified eclipsing binaries (KW Com and V1011 Her) whose periods appear not to have been previously published.

The details of these 68 objects are listed in Table 1; their folded SuperWASP lightcurves and power spectra are shown in Figure 1. Phase zero for each of the folded lightcurves is set at 2004 January 1st 00:00UT (i.e. HJD 2453005.5). The columns of Table 1 are as follows: 1. The number of SuperWASP objects which are duplicates, recorded with slightly different positions but displaying the same period, where this number is greater than one. 2. The SuperWASP identifier in the form '1SWASP Jhhmmss.ss+ddmmss.s'; the position encoded in this identifier will be identical to the position of the corresponding object in the USNO B1 catalogue. 3.

The *ROSAT* identifier either from the 1RXS or 2RXP catalogues. 4. The period in days as derived from the SuperWASP lightcurve. 5. The mean SuperWASP magnitude, defined as $-2.5 \log_{10}(F/10^6)$ where F is the mean SuperWASP flux in microVegas; it is a pseudo-V magnitude which is comparable to the Tycho V magnitude. 6. and 7. The B1 and R1 magnitudes respectively from the USNO catalogue (Monet et al. 2003). 8. A previously recorded name of the object. 9. The astronomical classification of the object. 10. The previously recorded period of the object. 11. A reference to the previous period determination.

The 68 previously classified periodic variables consist of 13 pre-main sequence stars, 10 Algol type (EA) eclipsing binaries (4 of which are also RS CVn stars), 5 β Lyrae type (EB) eclipsing binaries, 10 W UMa type (EW) eclipsing binaries, 6 BY Dra systems (5 of which also show UV Cet type behaviour, one of which has a white dwarf companion), 5 RS CVn systems (4 of which are also Algol type eclipsing binaries), 2 RR Lyrae stars, 15 Cepheid variables (13 of which were classified by the ROTSE project and one by the SAVS survey), one semi-regular pulsator, 3 cataclysmic variable stars, one supersoft source and one low mass X-ray binary.

The periods we have determined from our SuperWASP data for these known objects are generally in good agreement with previously published values (see Table 1). Where the periods differ significantly, we are confident that our determination is the more reliable measurement, owing to the better sampling of our data. In a couple of cases, for instance, we detect clear periodicities which are close to *half* that of objects discovered by ROTSE and claimed to be Cepheid variable stars. In another case, the cataclysmic variable PX And, the period we detect is the disc precession period rather than the binary orbital period of 0.14635d.

The remaining 360 objects comprise newly identified periodic variable stars which are also X-ray sources. Their details are listed in Table 2 and their SuperWASP lightcurves and power spectra are also shown in Figure 1. The columns of Table 2 are essentially the same as those in Table 1, without the previously determined periods and references, but with the addition of the spectral type where this is recorded in *SIMBAD*. Many of the objects in Table 2 are anonymous stars, with only a Hubble Space Telescope Guide Star Catalog or Tycho Catalog designation. Where objects have a designation other than one of these catalogue numbers, that is listed in Table 2. The period distribution of all 428 objects is shown in Figure 2.

In two cases (1SWASP J170033.82+200134.1 and 1SWASP J222229.09+281439.1) the SuperWASP lightcurves are double valued at all phases. In each case the objects are double stars (see Table 2) and the anomalous lightcurves are undoubtedly the result of one of the two stars (the non-variable one) sometimes appearing within the photometry aperture and sometimes not, so offsetting the mean brightness for a subset of the datapoints.

We also note that some folded lightcurves (e.g. that of 1SWASP J141630.88+265525.1) show regular ‘chunks’ of data (7 in this case) such that the measured period is close to the same integer number of days (i.e. the period is 6.9998d in the case of this object). However, although the phase coverage is uneven, these lightcurves cover many cycles of variation (121 days duration in the case of this object) and the period is reliable. The pattern seen is a result of the modulation period being close to an integer number of days and the sampling of the object repeating at the same time of night over many weeks. The longest period accepted for any object is less than half the data length in each case.

4. Discussion

4.1. Positional coincidence

As noted earlier, since the SuperWASP pixel size is relatively large ($13.7'' \text{ pixel}^{-1}$), the 2.5 pixel extraction aperture for photometry corresponds to $34''$ in radius. Given that the *ROSAT* sources can have positional uncertainties of up to tens of arcseconds, there is clearly the likelihood of chance positional coincidences between SuperWASP objects and catalogued X-ray sources.

The sky area covered by our 2004 Northern hemisphere observations is about 10^4 square degrees, and we have lightcurves of 6,713,217 objects from this SuperWASP run, of which 5,271,091 have more than 100 data points. The mean separation between nearest neighbours is therefore about $140''$ for the total set of SuperWASP objects. There are 14,616 *ROSAT* sources that fall within the sky area covered by our 2004 Northern hemisphere SuperWASP run, including 3,826 from 1RXS and 10,790 from 2RXP. (Many of these will, however, be duplicates between the two catalogues.) The mean error radius of the *ROSAT* positions is $18''$. Hence, there is a 5.3% chance of a given *ROSAT* source coinciding with one of our SuperWASP sources, purely at random. The fact that we find 4,562 matches, rather than the ~ 770 matches that would result from chance alone, suggests that at least $(4562 - 770)/4562 = 83\%$ of the positional coincidences are genuinely the result of X-ray emission from SuperWASP objects. At least 300 of the newly identified periodic variable stars identified here are therefore likely to be actual X-ray emitters.

4.2. Previously known periodic variable stars

The list of known variable stars in the sample considered here contains five accreting binary stars – the X-ray binary Her X-1, the supersoft X-ray source QR And, and the three cataclysmic variables PX And, V795 Her and DQ Her. These latter three are all magnetic CVs to some extent, and so have enhanced X-ray emission as a result.

Apart from this, the X-ray emission seen in the other objects with previously known periods is generally a result of stellar coronal activity (e.g. Rosner, Golub & Vaiana

1985; Hartmann & Noyes 1987). The key feature linking their X-ray emission is rapid rotation causing enhanced magnetic fields through the dynamo mechanism. This is particularly evident in the 13 pre-main sequence stars which we detect whose periods have been previously determined (e.g. from the COYOTE campaigns of Bouvier et al. 1993, 1995, 1997). These are young, rapidly rotating stars, and all those detected here are in the Taurus-Auriga star forming complex. We note that the observed photometric modulation periods of pre-main sequence stars are due to the presence of star spots, and that these can therefore change with time as spots appear and disappear at different latitudes. This will give rise to different modulation periods at different epochs if the stars rotate differentially (Neuhauser et al. 1995).

Another manifestation of coronal X-ray emission due to rapid rotation is in RS CVn stars. These are detached binary systems in which the rotation of the two components is locked to the orbital period of typically just a few days (Hall 1976; Strassmeier et al. 1993). One of the stars is usually a K sub-giant, and it is this star with its deep convection zone which develops a strong magnetic field and enhanced stellar coronal activity. Through optical selection effects, many RS CVn systems are detected as eclipsing binaries, and indeed we see that four of the five known RS CVn systems in this sample are of the Algol type, i.e. detached eclipsing binaries.

BY Dra stars are also well-represented amongst the systems with previously known periods. These are dwarf K or M stars showing emission lines and believed to be rapid rotators (Alekseev 2000; Strassmeier et al. 1993). Many of them show flare star behaviour and so are classed as UV Cet type stars too (Gershberg et al. 1999). The periods we see in the previously known systems of these types are almost certainly the rotation periods of the star. One of the previously catalogued BY Dra stars is V1092 Tau, which is a wide binary system containing a rapidly rotating K2V star and a hot white dwarf (Jeffries, Burleigh & Robb 1996).

Finally, we apparently see a surprising number of pulsating variable stars as X-ray sources. This includes both RR Lyr type, which are A or F giant stars with periods typically less than a day (Smith 1995), and δ Cep type (Cepheids) which are super-giants with periods of around 1 to 100 days (e.g. Turner & Burke 2002). Most of the apparent Cepheids recovered here were discovered by the ROTSE project. This detected 201 Cepheids in 2000 square degrees of sky coverage (Akerlof et al. 2000), giving a mean separation between them of 3.15° . There is therefore a chance of less than 0.001% that one of these ROTSE Cepheids would coincide with one of the *ROSAT* sources falling within the SuperWASP survey area. The fact that we find 13 ROTSE Cepheids coincident with *ROSAT* sources suggests that these objects are indeed X-ray emitters. However, whether they are actually Cepheid variables is not so certain.

Akerlof et al. (2000) classified ROTSE objects as Cepheids on the basis of having sinusoidal lightcurves and

periods in the range 1 to 50 days. However, there is no real evidence that these are likely to be Cepheids rather than other variables such as RS CVn systems. Objects such as ROTSE1 J172339.92+352759.3 and ROTSE1 J184633.30+485435.3 which we recover here are 11th magnitude stars with periods of ~ 24 d and ~ 5 d respectively. If they really were Cepheids, the period-luminosity relationship (Feast & Catchpole 1997) would place them at distances of 24.5 kpc and 11 kpc. Cepheids are Population I objects and therefore mostly lie in the Galactic disk. Since none of the objects we have considered here are in the Galactic plane, these distances are unrealistic. It is likely that *none* of the supposed ROTSE Cepheids we have detected as coincident with *ROSAT* sources are in fact correctly classified. The possibility of X-ray emission from pulsating stars was raised by Bejgman & Stepanov (1981) although there is little observational evidence in support of this other than a recent detection by *Chandra* of X-rays from the Cepheid Polaris (Evans et al. 2006). However, the observed X-ray to optical luminosity ratio of Polaris is many orders of magnitude smaller than the corresponding values of the supposed ROTSE Cepheids selected here (Engle, Guinan & Evans, 2006), providing further evidence of their misclassification.

In addition to discounting the ROTSE objects as true pulsating variables, the classification of SAVS J022708+342319 as a Cepheid is also uncertain (Maciejewski et al. 2004) and the RR Lyr variable HR Aur may be an active binary rather than a pulsating star (Loomis & Schmidt 1989). This leaves only V845 Her as a potential Cepheid with X-ray emission, but this appears to have H α in emission (Schmidt et al. 2004b). This too may be a sign of coronal activity and hence a misclassification.

4.3. Newly identified periodic variable stars

Amongst the newly identified periodic variable stars coincident with *ROSAT* sources, the majority are likely to be X-ray sources as a result of their rapid rotation. Indeed, 15 objects are previously identified as BY Dra stars, UV Cet stars, or other miscellaneous flare stars. We also see a further 30 previously catalogued pre-main sequence stars in this sample, which are likely to be rapid rotators too. We emphasise though that none of these 30 objects have previously been reported as showing coherent periodic variability. Within the set of 43 known young stars reported here (i.e. 13 with previously determined periods and 30 measured here for the first time), the distribution of periods found is quite broad: 7 have periods shorter than 1 d, 10 have periods between 1 d and 2 d, 13 between 2 d and 4 d, and 13 between 4 d and 10 d. We anticipate that the remaining, unclassified objects will contain further examples of these various classes of stars displaying rotational modulation.

Significant numbers of the newly identified objects are clearly eclipsing binaries with periods from a few hours

to a few days. We note though that in many cases, the period we have identified will be half the binary period, particularly in the case of W UMa type variables which display two minima of comparable depth. The newly identified X-ray emitting eclipsing binaries appear to include Algol type (e.g. 1SWASP 175540.63+372516.0 and 1SWASP J180331.30+080836.3), β Lyr type (e.g. 1SWASP J005101.78+200824.4 and 1SWASP J160248.22+252038.2) and W UMa type (e.g. 1SWASP J021208.77+270818.2 and 1SWASP J133538.39+491406.1) variables, as well as others which display more unusual morphology (e.g. 1SWASP J180207.45+183044.2). Many of these eclipsing binaries will contain tidally locked stars, so their components will also be rapid rotators displaying RS CVn type behaviour. This is likely to be the source of the X-ray emission in these cases too.

4.4. Flux ratios and modulation amplitudes

Given that X-ray activity in the majority of sources we have detected is expected to be linked to rapid rotation, one might expect to see an anti-correlation between X-ray emission and modulation period in our data. The modulation period may be the rotational period of a star, or a binary period, but tidal locking will make these periods identical for many close binaries, so preserving the correlation.

Previous studies have indeed shown strong correlations between X-ray emission and rotation period (e.g. Walter & Bowyer 1981; Pallavicini et al. 1981) but for very rapid rotation the X-ray luminosity is found to saturate at around 0.1% of the bolometric luminosity (e.g. Vilhu & Walter 1987; Wheatley 1998). Pizzolato et al. (2003) show that saturation occurs at rotation periods between 2 and 10 d depending on stellar mass.

In Figure 3 we plot ratios of X-ray to optical flux against our measured modulation periods. F_X is defined as the *ROSAT* count rate and F_O as the mean SuperWASP flux in microVegas. We do not attempt to calculate the more usual ratio of X-ray to bolometric luminosity because in most cases we do not have a sufficiently reliable measure of colour to estimate the spectral type and hence bolometric luminosity.

Figure 3 shows very little dependence of X-ray emission on modulation period. This indicates that, if the bulk of our sample are coronal emitters, they must be in the saturated regime. The lack of an obvious decrease in X-ray to optical flux even at periods longer than 10 d indicates that our sample is probably dominated by low mass stars ($M < 0.6 M_\odot$, Pizzolato et al. 2003). We find a very weak anti-correlation with $(F_X/F_O) \propto (P/\text{day})^{-0.14}$ and a value for the Pearson correlation coefficient squared of $R^2 = 0.02$. This may be due to the contribution of binaries containing giants and subgiants (Dempsey et al. 1993).

We further note that the known rapidly rotating isolated stars (BY Dra type, UV Cet type, pre-main sequence

stars etc) tend to lie at higher X-ray to optical flux ratios in this diagram, whilst the binary stars (eclipsing binaries and RS CVn stars) tend to lie at lower flux ratios. The relatively low observed X-ray to optical flux ratios of the RS CVn stars, when compared with the rapidly rotating single stars, may be due to the fact that we have not carried out any bolometric correction. The RS CVn stars will typically be K sub-giants, whilst the isolated rapid rotators are mostly M dwarfs, so their bolometric corrections will be different.

The five accreting binaries follow a different trend of increasing X-ray to optical flux ratio with period. In this case their X-ray emission is clearly not a result of enhanced coronal activity induced by rapid rotation. The cataclysmic variable PX And is detected here at its disc precession period (4.437d), if it were instead plotted at the position of its orbital period (0.146d) it would lie on the same trend as the other four accreting binaries in Figure 3.

Figure 4 shows a histogram of the X-ray to optical flux ratios in this sample of 428 objects, compared with the flux ratios of the other SuperWASP objects which are coincident with *ROSAT* objects but did not yield a modulation period from the period searching. Interestingly, the non-periodic sample shows a spread to larger X-ray to optical flux ratios than the periodic sample. These appear to be mostly coincident with galaxies or AGN, which are not expected to be periodic variables. However this sample will also contain periodic sources that are not strongly modulated, and others where the modulation period is not well sampled by the SuperWASP observations.

Figure 5 shows the modulation amplitude for our sample of 428 objects plotted as a function of modulation period. Here we see no correlation, other than to note that eclipsing binaries and RS CVn stars generally appear with higher modulation amplitudes than do the isolated rapidly rotating stars. Since most of the newly identified objects lie at lower amplitudes, this might indicate that the majority of these are likewise rapid rotators, rather than eclipsing binaries. However, we should also be mindful of selection effects which will mean that most of the previously identified eclipsing binaries will tend to be those with the deepest eclipses.

4.5. Colours

It is also instructive to plot the colours of this sample of objects, as this yields several interesting candidates for further investigation. Figure 6 shows the SuperWASP V – 2MASS K colour versus the 2MASS J – H colour of the objects. The solid line shows the approximate locus of the main sequence from around A0 to M6, for zero reddening. Every magnitude of V band extinction will shift this line upwards by 0.12 in (J–H) and to the right by 0.92 in (V–K), according to the extinction law of Wegner (1994). It is likely that the slight offset between the locus of the data points and the plotted main sequence is a result of the non-

standard V magnitude calculated from the SuperWASP unfiltered flux, and does not indicate any significant trend in these objects. The fact that most lie close to this zero-reddening main sequence suggests that the majority are relatively nearby objects. We note that four of the five accreting binaries (i.e. all except DQ Her) are amongst the bluest objects on this plot, whilst many of the pre-main sequence stars are amongst the reddest.

Looking first at the blue end of the colour-colour diagram, the two anonymous SuperWASP objects lying closest to the known accreting binaries are 1SWASP J132426.35+303314.2 (HD116635) with $P = 3.35$ d and 1SWASP J153633.39+271029.2 (SAO83906) with $P = 1.34$ d. Although neither have high X-ray to optical flux ratios, these objects warrant further investigation as potential accreting compact binaries. They are much bluer than their spectral classifications listed on SIMBAD (F and G respectively) would suggest.

The one previously classified rotational variable lying just above the accreting binaries with $(V-K) = 0.45$ and $(J-H) = 0.34$ is 1SWASP J034433.95+395948.0 which is positionally coincident with an anonymous pre-main sequence star listed on SIMBAD. The SuperWASP lightcurve clearly shows this object to be an eclipsing binary star with a period of 0.2888 d. Given its blue colour this is likely to be mis-classified and not a pre-main sequence star after all.

Moving to the red end of the colour-colour diagram, the one unclassified object lying above the main sequence amongst the very red pre-main sequence stars is 1SWASP J033025.95+310217.9 with $(V-K) = 4.63$, $(J-H) = 0.84$ and $P = 2.2308$ d. As this lies close to the previously catalogued pre-main sequence stars in the Taurus-Auriga star forming complex, this is likely to be another example of this class of objects, but previously uncatalogued.

The reddest of the previously classified binary stars is KW Com, with $(V-K) = 4.3$, which is listed in the GCVS as an eclipsing binary, although no period has previously been published. Its SuperWASP lightcurve is indistinguishable from many of the rotational lightcurves of the various pre-main sequence stars we have detected, and we therefore suggest it has been mis-classified in the GCVS and is really a young star displaying rotational modulation.

Although most of the unclassified SuperWASP objects lying at the red end of the colour-colour plot appear to be further examples of young stars displaying rotational modulation, there are some exceptions. In particular we note that there are four unclassified SuperWASP objects with $(V-K) > 3.4$, which therefore lie amongst the M stars, and which have lightcurves with a morphology that is suggestive of eclipsing binary stars. These are 1SWASP J142004.68+390301.5 with $P = 0.3693$ d and $(V-K) = 4.02$, 1SWASP J022050.85+332047.6 with $P = 0.1926$ d and $(V-K) = 3.93$, 1SWASP J220041.59+271513.5 with $P = 0.5235$ d and $(V-K) = 3.61$, and 1SWASP J224355.18+293647.6 with $P = 0.4443$ d and $(V-K) = 3.49$. These are likely to be low mass eclipsing bina-

ries, and representatives of a previously very poorly sampled population.

5. Conclusions

We have demonstrated the effectiveness of the SuperWASP survey for detecting photometric modulation on timescales of hours to weeks, in objects within the magnitude range $\sim 8 - 15$. As a result we have recovered the previously identified periodicities in 68 known variable stars coincident with *ROSAT* X-ray sources, and identified a modulation period for the first time in 360 more. By selecting on objects which are coincident with X-ray sources we have identified eclipsing binary stars and those showing rotational modulation, as well as picking out a few known accreting compact binary stars. We have shown that several previously catalogued pulsating variables coincident with *ROSAT* sources are likely to be misclassifications. Finally we have identified 4 objects as potential low mass eclipsing binaries on the basis of their lightcurve morphology and colours.

Acknowledgements. The WASP project is funded and operated by Queen's University Belfast, the Universities of Keele, St. Andrews and Leicester, the Open University, the Isaac Newton Group, the Instituto de Astrofísica de Canarias, the South African Astronomical Observatory and by PPARC.

This research has made extensive use of the SIMBAD database, operated at CDS, Strasbourg, France. We thank Harry Lehto for use of his implementation of the 1D CLEAN algorithm.

References

- anonymous, 2005, IBVS 5600
- Akerlof, C. et al, 2000, AJ, 119,1901
- Alekseev, I.Yu., 1998, Astronomy Reports, 42(5), 649
- Alekseev, I.Yu, 2000, Astronomy Reports, 44(10), 696
- Bejgman, I.L., Stepanov, A.E., 1981, SvAL, 7, 96
- Bouvier, J., Cabrit, S., Fernandez, M., Martin, E.L., Matthews, J.M., 1993, AA, 272, 176
- Bouvier, J., Covino, E., Kovo, O., Martin, E.L., Matthews, J.M., Terranegra, L., Beck, S.C., 1995, AA, 299, 89
- Bouvier, J., Wichmann, R., Grankin, K., Allain, S., Covino, E., Fernandez, M., Martin, E.L., Terranegra, L., Catalano, S., Marilli, E., 1997, AA, 318, 495
- Brancewicz, H.K., Dworak, T.Z., 1980, Acta Astronomica, 30(4), 501
- Brelstaff, T., 1991, Journal of the British Astronomical Association, 101(3), 171
- Chrastina, M., Szasz, G., Petrik, K., Hric, L., 2006, Open European Journal on Variable Stars, 23, 78
- Christian, D.J. et al, 2006, MNRAS, 372, 1117
- Clarkson, W.I. et al, 2007, in press
- Collier Cameron, A. et al, 2006a, MNRAS, 373, 799
- Collier Cameron A. et al, 2006b, MNRAS, 375, 951
- Deeter, J.E., Boynton, P.E., Miyamoto, S., Kitamoto, S., Nagase, F., Kawai, N., 1991, ApJ, 383, 324
- Dempsey, R.C., Linsky, J.L., Fleming, T.A., Schmitt, J.H.M.M., 1993, ApJ Supp., 86, 599
- Engle, S.G., Guinan, E.F., Evans, N.R., 2006, AAS, 209, 290

- Escola Sirisi, E., Garcia-Melendo, E., 1999, IBVS 4810
- Evans, N.R., Wolk, S.J., Guinan, E., Engle, S., Schlegel, E., 2006, AAS Meeting 208, 44.06
- Feast, M.W., Catchpole, R.M., 1997, MNRAS, 286, L1
- Gershberg, R.E., Katsova, M.M., Lovkaya, M.N., Terebizh, A.V., Shakhovskaya, N.I., 1999, AAS, 139, 555
- Hall, D.S. 1976, in IAU Colloq. 29, ed. Fitch, W.S, p287
- Hall, D.S., Kreiner, J.M., 1980, Acta Astronomica, 30(3), 387
- Hartmann, L.W., Noyes, R.W. 1987, ARAA, 25, 271
- Jeffries, R.D., Burleigh, M.R., Robb, R.M., 1996, AA,305, L45
- Kaiser, D.H., Lubcke, G., Williams, D.B., 1996, IBVS 4284
- Koen, C., Eyer, L., 2002, MNRAS, 331, 45
- Koppelman, M.D., West, D., Price, A., 2002, IBVS 5327
- Lister, T.A. et al. 2007, MNRAS, submitted
- Loomis, C.G., Schmidt, E.G., 1989, ApJ, 347, L77
- Maciejewski, G., Czart, K., Niedzielski, A., 2004, IBVS 5518
- Meinunger, L., Wenzel, W., 1968, Veroeffentlichungen der Sternwarte in Sonneberg, 7(4), 389
- Mironov, A.V., Moshkalev, V.G., Shugarov, S.Yu., 1983, IBVS 2438
- Monet, D.G. et al. 2003, AJ, 125, 984
- Neuhauser, R., Sterzik, M.F., Schmitt, J.H.M.M., Wichmann, R., Krautter, J., 1995, AA, 297, 391
- Pallavicini, R., Golub, L., Rosner, R., Vaiana, G.S., Ayres, T., Linsky, J.L., 1981, ApJ, 248, 279
- Pettersen, B.R., 1980, PASP, 92, 118
- Pizzolato, N., Maggio, A., Micela, G., Sciortino, S., Ventura, P., 2003, A&A, 397, 147
- Pollacco, D. et al, 2006, PASP, 118, 1407
- Pribulla, T., Kreiner, J. M., Tremko, J., 2003, Contributions of the Astronomical Observatory Skalnaté Pleso, 33(1), 38
- Qian, S.B., Zhu, L.Y., He, J.J., Boonruksar, S., 2003, New Astronomy, 8(5), 457
- Robb, R.M., 1989, IBVS 3346
- Robb, R.M., 1995, IBVS 4192
- Robb, R.M., Balam, D.D., Greimel, R., 1999, IBVS 4714
- ROSAT Consortium, 2000, ROSAT News, 72
- Rosner, R., Golub, L., Vaiana, G.S., 1985, ARAA, 23, 413
- Samec, R.G., Tuttle, J., Brougher, J.A., Moore, J.E., Faulkner, D.R., 1999, IBVS 4811
- Samus, N.N. et al, 2004, Vizier Online Data Catalog, 2250
- Schmidt E.G., Johnston, D., Langan, S., Lee, K.M., 2004a, AJ, 128, 1748
- Schmidt E.G., Johnston, D., Lee, K.M., Langan, S., Newman, P.R., Sneddon, S.A., 2004b, AJ, 128, 2988
- Selam, S.O., 2004, AA, 416, 1097
- Shevchenko, V.S., Grankin, K.N., Ibragimov, M.A., Melnikov, S.Ju, Yakubov, S.D., Chernyshev, A.V., 1991, IBVS 3652
- Smith, H.A., 1995, 'RR Lyrae Stars' Cambridge Astrophysics Series, Cambridge, New York. Cambridge University Press
- Stanishev, V., Kraicheva, Z., Boffin, H.M.J., Genkov, V., 2002, AA, 394, 625
- Strassmeier, K.G., Hall, D.S., Fekel, F.C, Scheck, M., 1993, AASS, 100, 173
- Street, R.A. et al. 2007, MNRAS, submitted
- Tamuz, O., Mazeh, T., Zucker, S. 2005, MNRAS 356, 1466
- Turner, D.G., Burke, J.F., 2002, AJ, 124, 2931
- Vilhu, O., Walter, F.M., 1987, ApJ, 321, 958
- Voges, W. et al, 1999, AA, 349, 389
- Voges, W. et al, 2000, IAUC 7432
- Walter, F.M., Bowyer, S., 1981, ApJ, 245, 671
- Wegner, W. 1994, MNRAS, 270, 229
- Wheatley, P.J., 1998, MNRAS, 297, 1145
- Zhang, E., Robinson, E.L., Stiening, R.F., Horne, K., 1995, ApJ, 454, 447

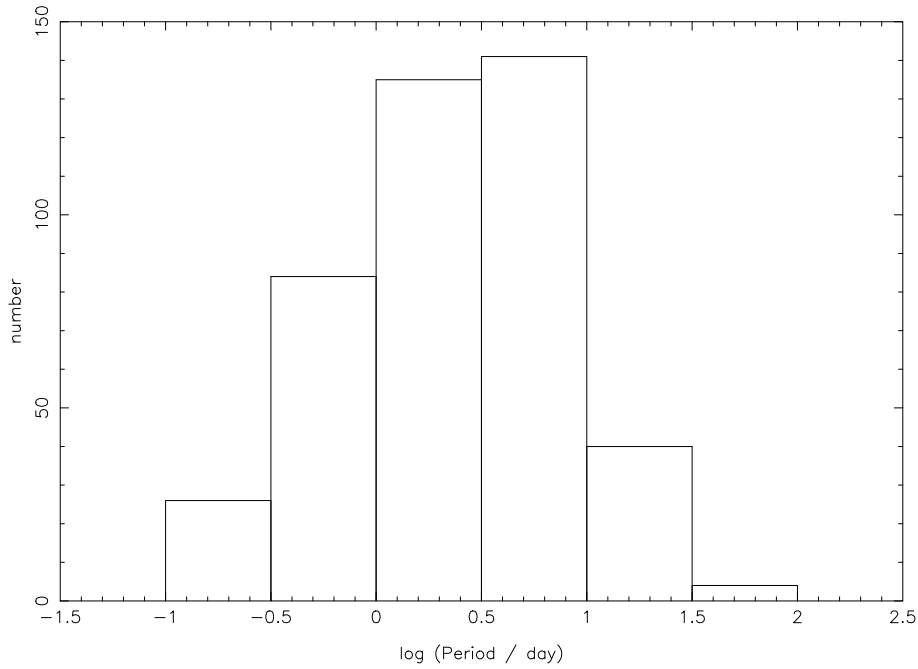


Fig. 1. The period distribution of our sample of 428 periodic variable stars coincident with *ROSAT* sources.

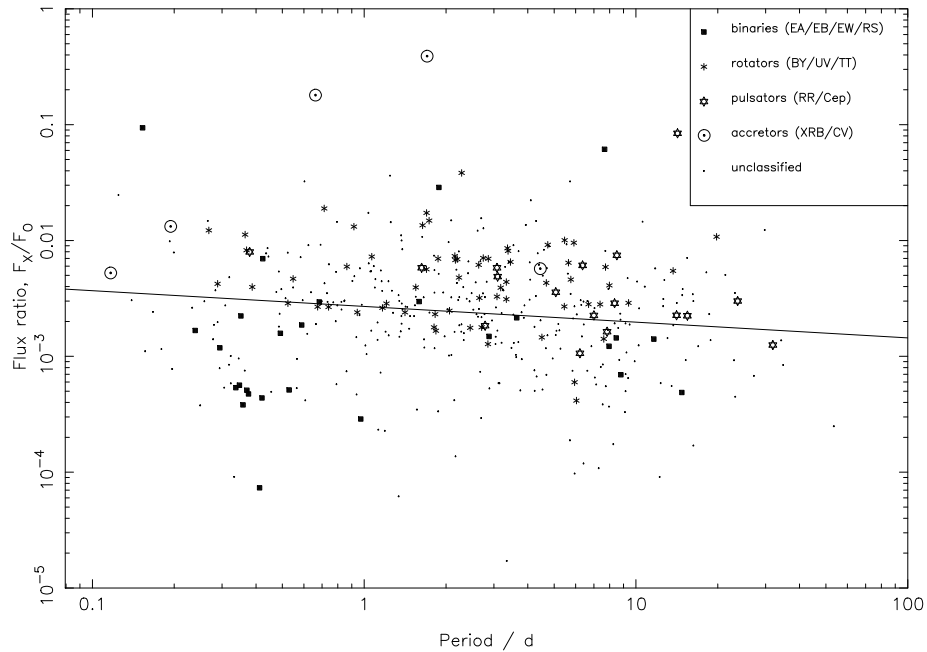


Fig. 2. The X-ray to optical flux ratio (calculated as the mean *ROSAT* count rate divided by SuperWASP mean flux) plotted against measured period for our sample of 428 periodic variable stars. The line shows the best-fit correlation defined by $F_X/F_O \propto (P/\text{day})^{-0.14}$. The symbols representing previously classified objects are shown in the inset key. ‘Binaries’ include Algol, β Lyr and W UMa type eclipsing binaries, as well as RS CVn stars; ‘rotators’ include BY Dra, UV Cet and pre-main sequence stars; ‘pulsators’ include those stars catalogued as either RR Lyr or δ Cep variables; ‘accretors’ include X-ray binaries and cataclysmic variables.

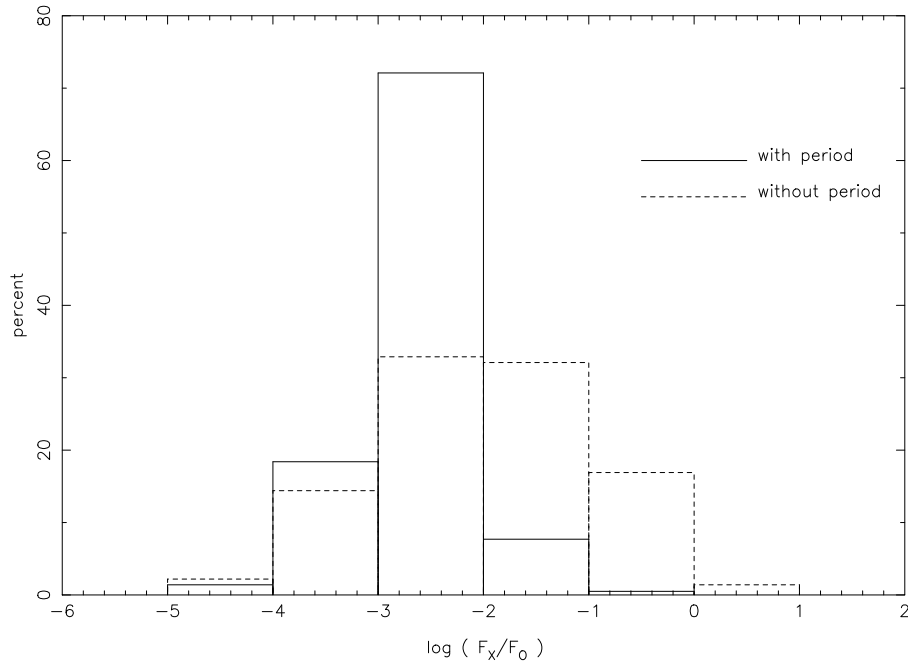


Fig. 3. The distribution of X-ray to optical flux ratio for all SuperWASP objects coincident with *ROSAT* sources. Both the sample of 428 objects displaying a period, and the remaining objects for which no period was found, are shown. Percentages are shown with respect to the individual sample size in each case.

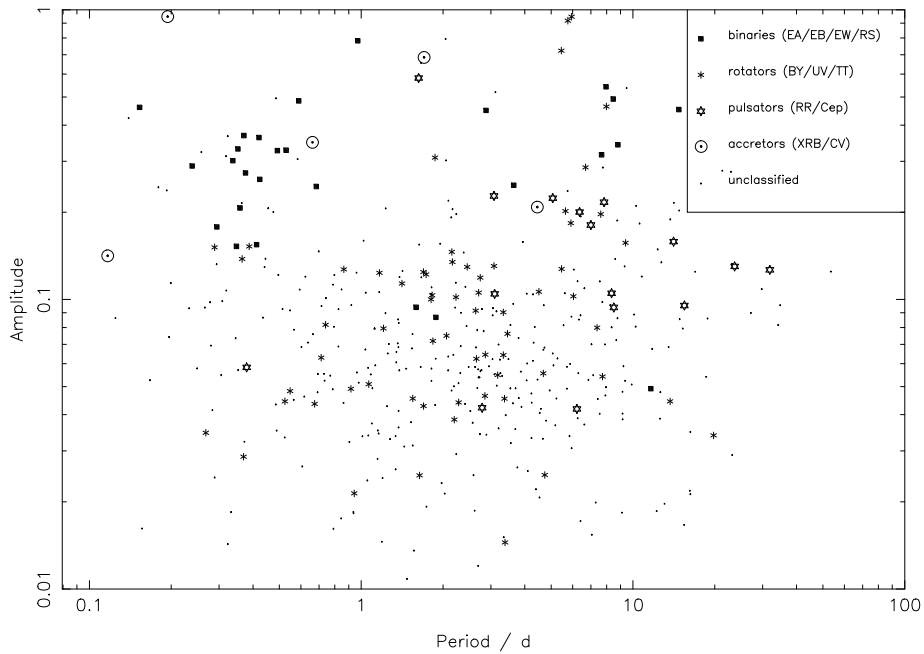


Fig. 4. The fractional modulation amplitude (calculated as the maximum flux minus minimum flux, divided by the maximum flux, measured from the folded and binned lightcurve) plotted against measured period for our sample of 428 periodic variable stars. No correlation is apparent. Symbols are as for Figure 3.

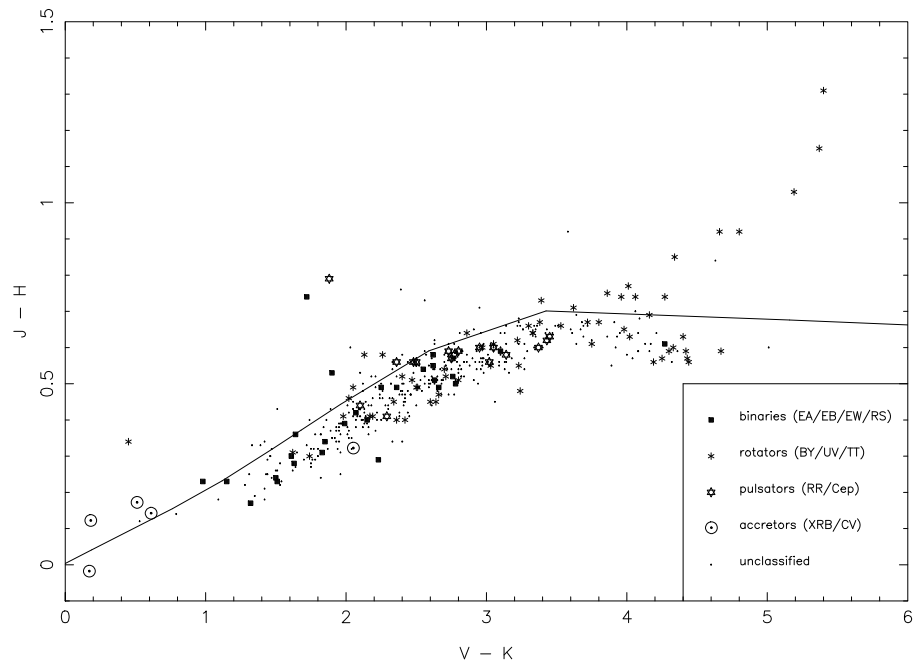


Fig. 5. The SuperWASP $V - 2\text{MASS } K$ colour plotted as a function of the $2\text{MASS } J - K$ colour for our sample of 428 variable stars. The accreting binaries are the amongst the bluest objects in this diagram, whilst some of the pre-main sequence stars are amongst the reddest. Symbols are as for Figure 3. The solid line shows the main sequence, for zero reddening, from A0 to late M.

Table 2: SuperWASP objects showing periodic variability, coincident with *ROSAT* sources, newly identified as periodic variable stars.

N	SuperWASP ID	<i>ROSAT</i> ID	Period/d	SW V	B1	R1	Name	Type	Sp
	J001357.58+350243.4	1RXS J001357.7+350233	2.5730	11.66	12.67	11.35			
	J001614.18+195144.2	1RXS J001614.0+195142	4.7901	11.01	13.08	7.88	LHS 107	double star	M4
	J001736.91+305119.2	2RXP J001737.2+305119	13.5338	12.49	12.91	11.66			
	J001825.00+232434.2	1RXS J001825.5+232432	1.5371	10.16	10.68	9.68	SAO 73880		G0
	J002001.09+275954.0	1RXS J002001.1+275949	4.6817	10.24	10.96	9.71	SAO73896		G5
	J002122.99+334237.1	1RXS J002123.2+334236	8.3490	11.01	11.80	9.84			
	J002334.66+201428.6	1RXS J002334.9+201418	7.9165	10.84	12.54	10.04	StKM 1-34		K5
	J003408.48+252349.7	1RXS J003408.7+252342	3.1555	11.11	13.00	10.37	BPM 84322		K5
	J004836.93+320859.2	2RXP J004836.7+320857	0.3054	12.64	13.23	11.92			
2	J005033.00+244902.0	1RXS J005033.3+244901	1.6968	11.48	14.01	14.96	LP 350-19/GJ 3060A	flare star	
	J005101.78+200824.4	1RXS J005101.5+200827	0.7966	11.77	12.75	11.04			
	J005515.01+301515.6	2RXP J005514.6+301517	4.0674	13.31	15.69	12.39			
	J005601.22+303825.9	2RXP J005601.2+303825	3.7947	12.88	12.44	10.55			
	J010705.51+190908.3	1RXS J010703.8+190858	1.3754	10.15	11.12	9.54			
	J011235.03+170355.7	1RXS J011235.6+170401	1.0362	13.55	15.30	12.92			
	J012139.75+253642.4	1RXS J012139.6+253634	0.5649	9.74	10.13	9.33	SAO 74655		F8
	J012215.44+202130.4	1RXS J012215.4+202139	10.2318	9.66	10.39	9.01			
	J012457.96+255702.4	1RXS J012458.8+255703	3.0420	10.75	11.40	10.29			
	J012757.37+185924.9	2RXP J012757.8+185931	0.7859	9.36	9.97	9.03	BD+18 193		F8
	J013147.20+384803.2	1RXS J013146.8+384757	8.7733	11.49	12.69	10.99			
	J013514.32+211622.4	2RXP J013514.3+211615	1.8710	10.97	11.58	10.49			
	J013612.29+304902.5	2RXP J013612.1+304901	0.6647	13.04	14.14	12.00			
	J013626.24+404343.8	1RXS J013625.8+404352	0.4357	12.59	14.07	11.41			
2	J013627.81+250835.5	1RXS J013628.0+250835	3.9346	11.02	12.53	10.48	BD+24 238	emission line star	K2e
	J013723.23+265712.1	1RXS J013723.4+265709	1.0852	10.95	13.02	9.96	StKM 1-174		K5
	J013727.14+390008.3	1RXS J013727.7+390000	1.0616	10.38	11.04	9.93			
	J014028.77+421200.8	1RXS J014028.6+421159	1.0605	10.61	11.46	9.81	BD+41 324		K0V
	J014453.62+282457.6	1RXS J014454.5+282440	1.1990	11.04	12.45	10.22			
2	J014633.48+331711.5	1RXS J014631.3+331715	4.9393	10.23	10.89	9.62			
	J015203.00+374808.7	1RXS J015201.5+374804	1.9530	11.53	11.90	10.96			
	J015548.02+242606.0	1RXS J015548.2+242620	3.2541	10.58	11.81	10.31			
	J015935.57+234852.6	1RXS J015935.7+234848	5.5569	12.54	13.37	11.38			
	J021208.77+270818.2	1RXS J021208.9+270817	0.3182	10.06	10.56	9.73			
	J022050.85+332047.6	1RXS J022050.7+332049	0.1926	12.91	14.47	11.80			
	J022133.29+340445.4	1RXS J022132.9+340449	3.6159	9.89	10.54	9.26	BD+33 411		G0
	J022452.45+422653.7	2RXP J022452.0+422654	2.0452	15.65	15.52	14.16			
2	J022729.25+305824.6	1RXS J022728.4+305828	13.6928	9.96	11.67	9.32	AG Tri	BY Dra	
	J022734.78+285830.2	1RXS J022733.2+285834	4.3104	9.89	10.51	9.40	SAO 75375		G0
	J022936.37+342343.1	1RXS J022936.5+342334	2.7458	12.20	13.65	11.76			
	J023503.81+313922.1	1RXS J023504.2+313927	1.2771	10.49	11.12	9.89	SAO 55677		G0
	J025020.65+372902.0	1RXS J025020.0+372909	1.7330	12.05	13.56	10.87		PMS star	K4V
	J025217.58+361648.1	1RXS J025216.9+361658	7.9809	11.18	12.09	9.89		PMS star	K2IV
	J025742.76+235744.5	1RXS J025740.5+235755	3.3348	10.11	9.37	8.19	AP Ari	PMS star	K0
	J025752.74+415135.1	1RXS J025755.5+415159	0.4854	12.06	13.16	10.52			
	J025828.76+294753.7	1RXS J025828.0+294805	0.6741	11.61	12.51	10.70		PMS star	K0IV
	J025953.10+380148.1	1RXS J025952.4+380149	0.3874	11.09	11.73	10.34		PMS star	K0IV
	J030335.64+362631.2	1RXS J030335.4+362635	8.2516	8.25	7.35	6.55	SAO 56117	double star	F8
	J030349.82+250234.0	1RXS J030349.4+250241	2.6754	11.89	13.62	10.94			
	J030405.14+300309.6	1RXS J030405.0+300312	1.8070	11.10	11.71	10.94		PMS star	K0V
2	J031531.89+260449.9	1RXS J031530.7+260451	9.3197	12.31	14.40	11.48			
	J032231.55+285319.8	1RXS J032231.4+285330	1.6648	10.76	11.48	10.43			
	J032714.41+272309.1	1RXS J032714.9+272318	10.0933	11.47	12.98	8.64	LP 300-3		
	J033025.95+310217.9	2RXP J033025.5+310215	2.2308	14.00	15.71	13.34			
	J033040.80+313658.1	2RXP J033040.9+313657	1.6559	11.88	13.33	11.64	BSD 47-661		K3V
	J033529.90+311337.4	2RXP J033529.9+311338	1.8366	9.21	9.55	8.59	SAO 56567	PMS star	G0
	J034057.81+311805.8	2RXP J034058.1+311802	4.2419	11.28	12.06	11.10			G1V
	J034145.61+271856.5	1RXS J034145.2+271855	2.6380	11.96	13.05	10.98	Wolf 1260	PMS star	K2IV
2	J034220.86+291440.9	1RXS J034221.6+291443	2.3271	10.67	12.49	11.14			
	J034348.34+250015.7	2RXP J034348.1+250008	0.4749	11.75	11.99	11.69	NSV 15748		
	J034433.95+395948.0	1RXS J034432.1+395937	0.2888	12.31	14.53	13.07		PMS star	K4V
2	J034450.16+321906.7	2RXP J034450.5+321909	6.0371	10.96	16.74	8.10	Dust Ball	PMS star	A0
	J034557.94+273335.2	1RXS J034557.2+273331	6.6237	10.94	12.21	10.23	HD 282932		K5
	J034630.44+330234.5	2RXP J034630.6+330238	1.1202	10.72	11.60	9.83	HD 278996		F
	J034906.11+234653.0	2RXP J034906.2+234652	0.3082	11.08	11.05	12.00			G9
	J034936.53+241745.8	2RXP J034936.3+241752	5.9466	11.97	12.49	10.88	V468 Tau	UV Cet	M3.7
	J034942.26+242746.8	2RXP J034942.2+242737	7.7479	12.27	13.48	11.39	NSV 1358		K3
	J035054.31+235005.5	1RXS J035055.0+235016	5.4490	11.76	12.44	10.99	V1176 Tau	BY Dra	
	J035208.32+241348.5	2RXP J035208.5+241343	1.6604	11.05	11.42	10.14	HD 283063		G5
	J035331.35+263141.1	1RXS J035330.5+263152	0.2835	12.13	12.71	11.16			G7IV
	J035425.23+242136.2	1RXS J035423.8+242146	2.2386	11.38	10.62	9.60	HD 283167		G5IV
	J035525.61+313047.9	2RXP J035525.1+313048	0.4856	12.98	14.29	12.11			
	J040005.79+394137.2	1RXS J040005.4+394133	5.6162	12.09	13.21	11.08			
	J040031.06+193520.8	1RXS J040030.7+193521	1.1677	10.44	11.51	9.74	HD 285281	PMS star	K0
	J040105.23+343902.9	2RXP J040105.2+343906	18.1451	10.73	11.77	10.23	HD 279311		K0
2	J040519.59+200925.5	1RXS J040518.6+200919	1.4406	10.55	11.27	9.57			
	J040753.30+335605.0	1RXS J040753.0+335555	3.8678	11.43	12.64	10.65			K3
	J040754.31+352749.2	1RXS J040753.8+352730	9.4797	10.45	11.54	9.75	HD 279444		G0
	J041327.27+281625.0	2RXP J041327.5+281623	0.8637	12.69	15.61	11.90	V1096 Tau	BY Dra	M0V
2	J041430.63+285129.8	2RXP J041431.0+285124	3.6916	11.15	14.17	11.26	V1097 Tau	emission line star	
	J041738.93+283300.7	2RXP J041739.1+283255	1.4127	13.26	15.57	13.12	LkCa5	PMS star	M2V
	J041810.78+231704.7	1RXS J041811.1+231700	1.8797	9.72	10.51	8.93	HD 284303		K0
2	J041831.11+281629.1	2RXP J041831.4+281636	5.7593	13.29	15.98	13.76	DD Tau	PMS star	K6V
	J041846.99+282008.2	2RXP J041847.0+282012	1.5483	12.00	14.31	11.21	V1023 Tau	PMS star	K7
	J041946.58+231748.4	1RXS J041946.0+231750	2.2176	10.82	11.68	10.25	HD 284296		G5
	J041953.70+300953.7	1RXS J041953.5+300949	10.2706	11.26	12.83	10.13	HD 281912		K0
	J042347.60+294038.2	1RXS J042346.8+294033	1.3836	11.51	12.73	11.52			K2
	J042521.02+254257.0	2RXP J042521.4+254252	7.6157	14.15	16.39	13.07	TAP34	PMS star	
	J042637.39+384502.3	1RXS J042638.5+384458	2.0596	11.04	11.72	10.24	HD 279788	PMS star	G5V
	J042937.53+232033.2	1RXS J042937.8+232032	4.5854	10.52	11.56	9.65	HD 284475	double star	K2
	J043049.18+211410.6	1RXS J043049.5+211356	0.7397	10.48	11.10	10.05	HD 284503	PMS star	G8
	J043114.43+271017.9	1RXS J043114.5+271021	5.9087	12.62	14.33	11.75	JH 56	PMS star	M1
2	J043230.55+241957.6	2RXP J043230.9+242002	6.6910	13.49	18.05	14.17	FY Tau	PMS star	
	J043547.33+225021.4	2RXP J043547.3+225027	2.4546	12.02	14.15	11.18	HQ Tau	PMS star	
5	J043554.15+225413.5	1RXS J043553.6+225410	1.2072	11.08	12.60	10.14	V1025 Tau	PMS star	

Table 2: continued.

N	SuperWASP ID	<i>ROSAT</i> ID	Period/d	SW V	B1	R1	Name	Type	Sp
	J155431.35+295652.1	1RXS J155430.9+295637	0.2328	11.46	12.46	11.35			
	J155842.13+323046.0	1RXS J155842.6+323047	6.2612	11.86	13.71	10.74			
3	J155850.50+272327.1	2RXP J155851.6+272333	34.2257	13.07	14.18	11.90			
	J160248.22+252038.2	1RXS J160248.3+252031	0.4955	10.71	11.55	10.16			
	J160351.74+423654.4	2RXP J160351.6+423650	0.7880	12.89	14.33	11.68			
	J160713.97+340136.0	1RXS J160714.4+340123	0.7418	10.91	12.11	10.46			
	J161213.07+341416.2	2RXP J161212.6+341411	0.6031	13.92	15.29	13.09			
	J162013.71+243611.0	1RXS J162013.2+243606	18.5948	9.74	10.76	8.95	SAO 84309		K0
	J162201.18+225021.6	1RXS J162200.9+225009	1.3728	11.83	13.70	11.10			
	J162255.30+224604.1	1RXS J162255.0+224559	1.7387	10.86	11.59	10.18			K
	J162641.33+335041.8	1RXS J162640.6+335033	23.1808	9.40	9.18	7.71	SAO 65302		G0
	J162946.59+281038.0	1RXS J162946.1+281034	1.4639	10.68	11.28	10.01			
	J163052.87+241224.3	2RXP J163052.5+241219	53.4764	10.80	11.79	10.00			
	J163420.90+424433.4	2RXP J163420.4+424426	0.3636	10.86	11.42	10.54			
2	J163527.45+350057.7	1RXS J163527.5+350046	0.9166	12.23	14.35	11.80	GJ 3966	flare star	M4
	J163739.45+221112.8	1RXS J163739.5+221104	2.0912	10.84	11.78	10.55			
	J163741.35+291950.4	1RXS J163741.2+291946	0.8246	11.43	12.70	10.82			
	J164159.14+363818.5	2RXP J164159.7+363819	12.2277	12.20	13.04	11.34			
3	J164732.08+251938.5	1RXS J164732.3+251931	0.9048	11.50	13.27	10.78			
	J164942.92+222003.7	1RXS J164943.4+222009	22.9494	10.34	11.83	9.37			
	J164956.83+325235.6	1RXS J164955.5+325232	1.0396	11.98	13.61	11.23			
	J164959.95+412225.9	1RXS J165000.2+412217	1.8137	11.24	12.43	10.50	AG+41 1420		K0
	J165025.84+272817.2	1RXS J165027.1+272812	2.2815	11.32	11.95	11.12			
	J165107.29+283601.0	1RXS J165107.2+283601	16.1973	11.44	13.83	10.87	StKM 1-1407		K7
2	J165211.93+202138.7	1RXS J165212.4+202148	3.6987	12.43	14.67	11.25			
	J165445.06+423227.5	1RXS J165445.3+423237	0.6912	13.02	14.57	12.82			
	J165820.66+333353.2	1RXS J165819.2+333411	4.5302	9.81	10.52	9.35			
	J165909.65+205816.4	1RXS J165909.5+205807	4.1037	11.90	14.26	10.89			
	J165921.89+342822.4	2RXP J165921.7+342822	1.5636	10.79	11.17	10.29			
	J170033.82+200134.1	1RXS J170032.9+200137	4.2298	9.95	11.37	9.56	SAO 84750	double star	G5
	J170303.06+320325.8	1RXS J170303.1+320320	2.7718	11.48	12.07	10.87	BD+32 2836		F8
	J170313.51+245321.0	1RXS J170313.2+245332	5.8417	10.14	10.67	9.50			
	J170352.84+321145.7	1RXS J170352.9+321147	15.4221	11.27	13.01	11.43	NLTT 44114		M3
	J171733.62+495515.7	2RXP J171733.8+495513	2.0939	13.87	14.76	14.04			
	J171800.30+212809.4	1RXS J171800.1+212816	0.7904	10.08	10.55	9.66			
2	J171808.56+250612.0	1RXS J171807.5+250610	2.4103	10.71	11.97	10.21	BD+25 3238		M0
	J171921.10+480342.8	2RXP J171921.7+480338	5.9483	9.75	10.39	9.28	SAO 46635		G5
2	J171954.21+263003.0	1RXS J171953.4+262958	19.8077	10.65	13.05	10.49	V647 Her	UV Cet	M4eV
	J171959.47+241205.6	1RXS J171959.4+241202	0.7129	13.35	15.65	13.43	V475 Her	UV Cet	
	J172011.53+495456.0	2RXP J172011.4+495454	0.9353	11.57	12.09	11.15			
	J172158.32+574922.2	1RXS J172157.8+574913	6.4272	11.11	11.74	10.78			
	J172228.64+365842.1	1RXS J172228.5+365843	1.2283	10.63	11.99	10.15	StKM 1-1466		K5
	J172314.19+283650.3	1RXS J172314.4+283641	3.8881	10.85	11.66	10.62			
	J172413.67+402617.2	1RXS J172413.5+402616	0.2890	11.38	12.27	10.55			
	J172524.34+504212.2	2RXP J172522.4+504216	0.5137	14.65	16.03	14.80			
	J173004.97+184339.3	1RXS J173004.9+184340	12.6078	10.69	11.37	10.09	BD+18 3387		K0
	J173103.32+281506.5	1RXS J173103.4+281510	1.2653	10.27	11.07	9.72			
	J173216.05+484750.1	1RXS J173216.5+484754	12.7178	12.39	13.83	12.48			
3	J173335.83+204847.4	1RXS J173336.7+204847	7.0610	10.29	11.45	9.68			
	J173353.14+165512.8	1RXS J173353.5+165515	0.2659	13.04	16.14	13.93			
	J173636.82+151508.3	1RXS J173637.6+151511	2.6726	10.34	10.90	9.91			
	J173658.21+300947.5	1RXS J173657.6+300943	5.1781	11.00	11.88	10.61			
	J173659.28+485946.1	1RXS J173658.9+485931	2.6143	12.72	14.72	12.49	StKM 1-1501		K4
	J173733.44+414619.9	1RXS J173734.1+414618	1.5480	11.16	12.25	10.86			
	J174431.65+131257.5	1RXS J174432.1+131259	2.7015	11.44	12.77	10.34			
2	J174625.25+222859.5	1RXS J174624.9+222851	3.5384	11.08	11.75	10.52			
	J174705.04+332129.1	1RXS J174704.1+332126	3.2041	11.60	12.53	10.94			
2	J174746.93+521340.2	1RXS J174745.8+521355	2.9532	11.42	12.26	11.18			
	J174903.15+230745.5	2RXP J174903.8+230744	16.9438	11.73	12.64	10.55			
	J174947.04+335059.1	1RXS J174947.6+335056	1.3479	10.90	11.49	10.05			
	J174951.66+232807.3	2RXP J174951.9+232759	2.1447	9.95	10.39	9.53	SAO 85451		F8
	J175133.95+414127.4	1RXS J175133.3+414121	9.3576	9.97	11.22	9.29	BD+41 2912		K0
	J175141.38+281901.2	1RXS J175140.9+281855	2.6946	13.02	14.67	12.92			K
	J175152.94+093751.8	2RXP J175153.4+093753	9.1586	10.86	11.89	10.73			
	J175216.36+093757.5	2RXP J175216.1+093748	7.2957	10.02	10.59	9.36			
	J175242.72+232728.9	1RXS J175242.3+232724	3.0911	10.22	11.28	9.74	BD+23 3201	double star	
	J175319.15+213029.5	1RXS J175318.5+213028	10.7768	10.89	12.31	10.54			
2	J175540.63+372516.0	2RXP J175539.5+372516	3.1203	12.94	13.57	12.72			
2	J175711.41+224706.3	1RXS J175711.2+224712	1.8139	11.74	12.65	11.19	StKM 1-1560		K7
	J175718.89+313315.9	1RXS J175718.5+313314	0.6981	10.79	11.33	10.12			
	J175734.12+584414.2	1RXS J175733.7+584414	3.2408	11.96	13.76	10.86			
	J175758.92+550607.7	1RXS J175758.9+550608	0.6374	11.20	11.85	10.60			
2	J175809.40+092240.8	1RXS J175809.3+092241	0.4885	10.90	11.79	10.38			
	J175910.35+584259.4	1RXS J175910.1+584300	1.2314	11.00	11.68	10.63			
2	J175954.36+104418.9	1RXS J175953.7+104402	5.8737	10.91	11.97	10.20			
	J180029.35+510008.8	2RXP J180028.5+510002	1.1913	10.04	10.41	9.56	SAO 30688		F8
	J180100.51+233945.4	1RXS J180100.0+233936	14.8666	10.77	11.72	10.09	HD341448		K0
	J180207.45+183044.2	1RXS J180208.6+183043	0.5477	11.66	13.44	11.41			
	J180238.80+335634.6	1RXS J180239.2+335639	7.4245	9.62	10.24	9.13	SAO 66576		G5
	J180331.30+080836.3	2RXP J180331.2+080832	2.0523	12.07	12.17	11.45			
	J180426.56+393047.1	1RXS J180426.3+393044	1.5451	11.84	13.25	10.98			
	J180500.38+111013.9	2RXP J180500.8+111021	0.6070	11.02	11.32	10.57			
	J180514.38+113148.6	2RXP J180514.3+113143	2.7255	13.08	13.89	11.88			
	J180525.04+175729.7	2RXP J180525.1+175725	27.1661	11.45	12.19	11.06			
	J180859.30+454910.7	2RXP J180859.1+454927	6.0582	11.37	15.40	14.01			
	J181004.20+090620.8	2RXP J181004.1+090622	0.8470	14.11	15.76	13.55			
	J181306.46+260151.9	1RXS J181306.1+260145	2.2838	12.77	14.93	12.64	GJ 4044	flare star	M4
	J181350.48+134936.6	2RXP J181350.4+134937	2.6248	13.68	15.55	13.24			
3	J181538.78+381949.9	1RXS J181537.9+381927	3.1452	9.79	10.68	9.47			
	J181725.16+482201.8	1RXS J181725.6+482202	16.2578	10.91	13.89	10.77			
	J181938.10+364059.2	1RXS J181937.8+364057	1.0536	11.40	12.77	10.83			
	J182131.56+233430.7	1RXS J182130.8+233434	1.0945	11.51	12.42	10.76	HD 342009		K0
	J182247.09+443442.9	1RXS J182247.1+443442	5.7509	11.52	12.92	10.57			
	J182850.26+350634.3	1RXS J182849.7+350637	2.6940	9.18	9.57	8.66	SAO 67013		G5
	J182934.89+295804.5	1RXS J182935.0+295807	0.8610	8.92	8.74	7.86	SAO 86121	double star	F8/F5
	J183018.86+344656.4	1RXS J183018.1+344633	3.0479	10.78	11.28	10.12			

Table 2: continued.

N	SuperWASP ID	<i>ROSAT</i> ID	Period/d	SW V	B1	R1	Name	Type	Sp
	J183037.25+433553.2	1RXS J183037.6+433555	23.1356	11.39	12.62	11.82			
	J183544.62+300814.7	1RXS J183544.4+300808	0.6175	11.06	11.57	10.29			
	J183956.25+510534.0	1RXS J183956.7+510532	6.8528	9.01	8.49	7.52	SAO31094	double star	G5
	J202823.91+113110.9	1RXS J202823.9+113115	1.0209	10.02	10.40	9.47			
	J202932.83+122730.8	1RXS J202932.3+122735	3.7553	9.95	10.42	9.40			
2	J203553.02+100611.9	1RXS J203552.3+100555	0.9644	12.44	14.09	12.68			
	J203621.99+121539.4	1RXS J203622.0+121519	12.3366	9.77	10.89	8.91			
2	J203904.65+233847.2	1RXS J203905.4+233845	0.7145	12.28	13.65	11.35			
	J204017.10+143035.6	1RXS J204018.3+143030	0.9378	9.86	10.12	9.38			
2	J204404.76+131412.1	1RXS J204404.5+131413	2.1510	10.71	11.34	10.09			
	J204853.35+122230.3	1RXS J204853.6+122219	6.2897	10.77	11.71	10.32	BD+11 4390		G5
	J204922.85+064739.2	1RXS J204924.0+064737	9.1662	10.33	10.84	9.57	BD+06 4654		F
	J205428.00+090606.6	1RXS J205428.0+090615	2.2374	11.73	12.80	10.58			
	J210124.59+054212.8	1RXS J210124.1+054207	0.9801	11.71	12.50	11.07			
2	J210144.82+100840.7	1RXS J210145.1+100843	13.0611	9.85	10.77	9.18	SAO 126476		K2
	J210707.11+063232.1	1RXS J210707.1+063247	7.1371	10.04	10.70	9.54			
	J211044.78+162323.7	1RXS J211044.8+162312	10.5750	12.34	13.62	11.26			
	J211436.75+195255.7	1RXS J211437.1+195257	1.1520	11.87	13.50	11.13			
	J212135.86+094835.3	1RXS J212136.2+094834	3.6237	10.55	11.24	9.76			
	J212341.65+152148.1	1RXS J212342.2+152151	6.6225	10.37	11.42	10.10			
2	J212519.57+265653.8	1RXS J212519.7+265657	2.8246	11.26	12.20	11.11			
	J212812.94+075227.2	1RXS J212813.2+075229	29.7822	12.72	13.90	11.49			
	J212846.86+232012.5	1RXS J212846.4+232009	4.5407	11.15	12.69	10.38	StKM 1-1900		K4
2	J212934.76+093530.3	1RXS J212935.1+093522	2.7362	11.71	12.71	10.51			
	J213004.12+120428.8	2RXP J213005.4+120426	0.5837	15.23	15.49	14.61			
	J213116.74+225357.1	2RXP J213116.9+225402	1.1268	10.05	10.67	9.71			
	J213221.70+243342.4	1RXS J213220.8+243337	4.7358	11.99	13.98	11.22	GJ 4201	flare star	M3.5
	J214537.36+271110.8	1RXS J214539.0+271124	1.3729	11.30	12.25	11.00			
	J214742.17+304210.5	1RXS J214741.8+304204	34.7828	10.25	11.62	9.37	BD+30 4528		K2
2	J214809.40+191012.9	1RXS J214810.6+191013	1.1598	10.64	11.83	10.04			
	J214916.06+312502.5	1RXS J214916.6+312500	6.4128	10.82	11.54	10.49			
	J215323.65+173020.3	2RXP J215323.6+173019	5.2761	13.00	13.50	12.04			
	J220041.59+271513.5	1RXS J220042.0+271520	0.5235	11.37	13.06	10.57			K
	J220213.95+152014.2	1RXS J220212.8+152012	1.4751	9.74	10.72	9.37			
2	J220406.39+343305.3	1RXS J220407.2+343309	0.3717	9.90	10.26	9.63	BD+33 4417	double star	F5
	J221844.11+142130.2	2RXP J221844.4+142132	4.7004	13.13	13.59	11.89			
2	J222228.81+292212.4	1RXS J222228.4+292216	0.2779	10.44	11.43	10.12			
4	J222229.09+281439.1	1RXS J222229.1+281432	2.2761	9.34	10.66	9.46	SAO 90449/SAO 90450	double star	G0/F8
	J222558.19+210842.0	2RXP J222558.7+210837	5.0987	13.23	14.16	12.61			
	J222614.44+213209.6	2RXP J222613.9+213219	2.8894	9.94	9.36	8.33	BD+20 5152		K0
	J222629.93+212314.5	2RXP J222629.8+212318	1.0101	12.77	14.25	12.20			
	J222803.99+183606.5	1RXS J222804.5+183607	0.3232	9.97	10.35	9.72	BD+17 4751		F8
	J222820.71+173959.3	1RXS J222819.9+174025	2.3142	12.02	13.38	11.92			
	J222829.08+203637.0	1RXS J222834.4+203647	0.1247	13.27	13.99	12.49			
	J223616.76+331856.7	1RXS J223616.0+331909	0.3230	10.66	11.20	10.21			
	J223655.17+401027.8	2RXP J223655.4+401024	15.2555	11.42	12.18	10.87			
	J224355.18+293647.6	1RXS J224353.3+293633	0.4443	12.54	14.15	11.42			
	J224446.13+302933.6	1RXS J224446.2+302927	3.5533	10.40	11.07	9.80			
2	J225155.50+353915.2	1RXS J225155.6+353911	5.2276	11.03	12.24	10.69			
	J225338.13+291305.0	2RXP J225337.7+291310	0.8252	12.33	12.74	11.28			
	J225454.99+241445.2	1RXS J225453.7+241449	0.1994	12.70	15.68	12.91			
2	J225538.93+281035.2	1RXS J225537.7+281051	0.8442	11.77	12.60	11.44			
	J225617.59+205236.2	2RXP J225617.9+205236	1.0999	11.60	12.84	10.95			
2	J225849.98+405611.4	1RXS J225850.4+405610	6.3266	10.86	11.66	10.34			
	J225923.53+325133.3	1RXS J225923.2+325127	2.3833	11.90	12.98	11.24			
	J230147.77+352848.3	1RXS J230147.6+352854	14.1358	9.74	10.86	9.03	SAO 72938		K2
2	J230209.26+351539.4	1RXS J230209.2+351538	9.1534	10.05	11.01	9.51			
	J230724.88+315014.1	1RXS J230725.0+315012	7.7129	10.67	12.08	9.73			
	J230843.02+213717.7	1RXS J230842.4+213716	7.5465	9.40	10.11	8.80	SAO 91038		G5
	J231036.91+205526.2	1RXS J231037.8+205531	0.9198	10.16	10.87	9.37	HD 218782		K2
	J231059.54+214243.2	1RXS J231100.1+214254	0.2582	11.22	12.51	11.01			
2	J231206.52+265545.7	1RXS J231206.8+265552	0.1563	9.37	13.10	7.39	HDS 3305	double star	K3
	J231455.84+273958.5	1RXS J231456.5+273957	11.7668	11.59	12.62	10.52			
	J232048.10+292155.6	1RXS J232048.8+292151	1.3710	11.52	11.97	10.86			
2	J232153.08+231656.2	1RXS J232153.8+231703	18.8148	10.90	11.59	10.43			
	J232617.06+275203.5	1RXS J232617.4+275200	1.2530	11.72	13.67	11.11			
4	J233152.17+195614.2	1RXS J233152.6+195735	1.0664	9.63	12.12	9.55	EQ Peg	UV Cet	M3.5
	J233906.78+220412.4	1RXS J233907.3+220355	4.0623	10.55	11.42	9.79	BD+21 4966		K2
	J234028.98+295911.8	1RXS J234027.8+295912	1.1648	11.16	10.48	8.90			
	J234106.15+270643.2	2RXP J234106.2+270638	9.8987	11.95	12.79	10.77			
	J234720.80+300510.8	1RXS J234721.7+300505	2.3252	10.81	11.49	10.41			
	J234945.36+312627.4	1RXS J234944.9+312629	1.3808	12.77	13.56	11.60			
	J235750.15+334348.5	1RXS J235750.3+334401	1.4194	11.21	12.66	10.96			
	J235952.73+294947.3	2RXP J235952.7+294949	0.5657	13.22	13.70	12.15			